Nano Research
DOI 10.1007/s12274-017-1561-z
Research Article
ISSN 1998-0124
CN 11-5974/O4

Anionic liposomes for small interfering ribonucleic acid (siRNA) delivery to primary neuronal cells: Evaluation of alpha-synuclein knockdown efficacy

Michele Schlich[1], Francesca Longhena[2], Gaia Faustini[2], Caitriona M. O'iscoll[3], Chiara Sinico[1], Anna Maria Fadda[1], Arianna Bellucci[2], and Francesco Lai[1] (✉)

[1] *Department of Life and Environmental Sciences, University of Cagliari, Cagliari 09124, Italy*
[2] *Division of Pharmacology, Department of Molecular and Translational Medicine, University of Brescia, Brescia 25123, Italy*
[3] *Pharmacodelivery Group, School of Pharmacy, University College Cork, Cork, Ireland*

Received: 22 November 2016
Revised: 23 February 2017
Accepted: 26 February 2017

KEYWORDS
rabies virus glycoprotein (RVG) peptide,
liposomes,
small interfering ribonucleic acid (siRNA),
alpha-synuclein,
primary neuronal cells,
Parkinson's disease

ABSTRACT

Alpha-synuclein (α-syn) deposition in Lewy bodies (LB) is one of the main neuropathological hallmarks of Parkinson's disease (PD). LB accumulation is considered a causative factor of PD, which suggests that strategies aimed at reducing α-syn levels could be relevant for its treatment. In the present study, we developed novel nanocarriers suitable for systemic delivery of small interfering ribonucleic acid (siRNA) that were specifically designed to reduce neuronal α-syn by RNA interference. Anionic liposomes loaded with an siRNA–protamine complex for α-syn gene silencing and decorated with a rabies virus glycoprotein (RVG)-derived peptide as a targeting agent were prepared. The nanoparticles were characterized for their ability to load, protect, and deliver the functional siRNA to mouse primary hippocampal and cortical neurons as well as their efficiency to induce gene silencing in these cells. Moreover, the nanocarriers were evaluated for their stability in serum. The RVG-decorated liposomes displayed suitable characteristics for future *in vivo* applications and successfully induced α-syn gene silencing in primary neurons without altering cell viability. Collectively, our results indicate that RVG-decorated liposomes may be an ideal tool for further studies aimed at achieving efficient *in vivo* α-syn gene silencing in mouse models of PD.

1 Introduction

Alpha-synuclein (α-syn) is a 140 amino acid protein abundantly expressed throughout the central nervous system (CNS) [1]. The protein is crucially involved in the regulation of neurotransmitter trafficking at the pre-synaptic region, where it exists in equilibrium between a soluble and a vesicle-bound form [2]. In

Address correspondence to frlai@unica.it

particular, α-syn has been found to interact with synaptic vesicles as well as pre-synaptic membrane-associated proteins [3–5]. However, α-syn knockdown and null mice were viable, fertile, and had normal motor behavior, suggesting that a compensative effect exists with the other forms of synucleins (β and γ) [6, 7].

In 1997, α-syn was identified as the main protein component of Lewy bodies (LB) [8], eosinophilic inclusions that are among the main pathological hallmarks of Parkinson's disease (PD), PD dementia (PDD), dementia with Lewy bodies (DLB), LB variant of Alzheimer's disease (AD) and LB dysphagia. There is evidence that the deposition of the protein in the brain plays a pathogenic role in these disorders. Indeed, mutations and multiplications of the α-syn gene locus SNCA cause the onset of familial forms of PD and DLB, and the progression of PD symptoms correlate with the topographical spreading of LB pathology in the brain [9]. Furthermore, studies of experimental models of PD have shown that α-syn accumulation and aggregation is neurotoxic, thus corroborating the aforementioned observations [5].

Thus, since clinical and experimental findings indicate that higher levels of α-syn promote its toxic potential [10, 11], it is also reasonable to postulate that neuroprotective effects could be achieved by suppressing this protein expression in neurons.

In the last decade, ribonucleic acid (RNA) interference (RNAi) has been a useful tool to reduce the expression of α-syn *in vitro* and *in vivo* through the administration of small interfering RNA (siRNA) or short hairpin RNA (shRNA) vectors. An shRNA-expressing lentiviral vector designed to silence human α-syn has been found to efficiently knock down the target protein both *in vitro* in the human SH-SY5Y cell line and *in vivo* in the striatum of human α-syn transgenic rats [12]. Nevertheless, the clinical use of viral vectors is hindered by the risk of immunogenicity and issues linked to large-scale production [13]. As an alternative, the use of naked siRNA was exploited to achieve specific and resilient silencing of α-syn in the hippocampus and cortex of mice after intracerebral infusion [14]. More recently, the potential of α-syn silencing was investigated in non-human primates. Indeed, a chemically modified siRNA administered to the left substantia nigra of squirrel monkeys was found to induce a significant gene knockdown of the protein without triggering adverse reactions at the injection site [15]. Conversely, other researchers detected dramatic neurotoxicity following intrastriatal infusion of adenoviral vectors embedded with SNCA shRNA and a sudden drop of tyrosine hydroxylase (TH)-positive cells and dopamine levels at 4 weeks after administration [16]. Based on these results, it is hypothesized that a "therapeutic window" of α-syn silencing may exist in which insufficient or excessive expression levels lead to toxicity. Another possible explanation for these results may rely on the fact that adenoviral vector injections can induce strong neuroinflammatory and immune cell activation [17]. These pathways could certainly contribute to the induction of noxious events that, coupled with the neuropathological alterations occurring in the injured brain of PD animal models, may transform α-syn gene silencing from beneficial to detrimental. Therefore, non-viral delivery of siRNA, rather than viral vector-associated shRNA delivery, seems to provide a more promising and safer route to investigate gene silencing in the human brain. This is reinforced by the fact that the use of shRNA can be associated with a broad spectrum of off-target irreversible effects on gene regulation [18].

Nonetheless, when focusing on the potential clinical translation of siRNA therapeutics to neurological disorders, the route of administration is of primary importance. In this regard, the previously cited works, although demonstrating the therapeutic potential of α-syn siRNAs, lack an acceptable application route for the treatment of a large population of human patients, as the associated gene silencing is temporary and could only be achieved through intracerebral infusion. Instead, brain-targeted delivery of siRNA by systemic administration (e.g., intravenous) would provide a non-invasive alternative with greater patient acceptability, reduced cost, and without the risks associated with surgery.

However, the fascinating potential of brain delivery after systemic administration of siRNA is undermined by limitations derived from the difficulties of crossing the blood–brain barrier (BBB) as well as from the unfavorable physicochemical characteristics of siRNA. In fact, siRNA is double-stranded RNA and is hydrophilic and anionic in nature, so it is unsuitable for

permeability across both cell membranes and the BBB [19]. In addition, quick degradation by circulating ribonucleases (RNAses) and fast renal elimination result in an extremely short (< 5 min) plasma half-life [20]. For this reason, several nanocarriers of different nature (polymeric, lipidic, peptidic, and so on) have been recently used as siRNA-encapsulating agents to improve *in vivo* stability and targeted organ delivery [21, 22].

For instance, Cooper et al. included an anti-SNCA siRNA in exosomes whose surfaces were decorated with a rabies virus glycoprotein-derived peptide (RVG peptide) [23] that is known to function as a brain delivery agent. Indeed, the RVG peptide can bind the acetylcholine receptors on brain endothelial cells and trigger a receptor-mediated transcytosis that allows the nanocarrier to cross the BBB and results in widespread delivery in the brain parenchyma [24, 25]. RVG-modified exosomes efficiently decreased the levels of endogenous and pro-aggregating α-syn after systemic administration in wild type (wt.%) or transgenic mice, respectively. In addition, the use of exosomes as drug delivery systems has been shown to hold great potential, especially for their intrinsic ability to mediate cell-to-cell material transfer and their enhanced stability in circulation. However, the variability in size and composition due to different cellular origins, the risk of immune suppression or activation, and the lack of large-scale isolation methods represent major obstacles for the clinical translation of exosomes as siRNA delivery vectors [26, 27].

Liposomes are the synthetic counterpart of exosomes and share with them the vesicular structure formed by a phospholipid bilayer. In addition, the external surface of liposomes can be chemically modified to introduce a targeting agent to trigger the penetration of the BBB through receptor-mediated transcytosis [28]. Cationic liposomes can bind siRNA by electrostatic interactions to form lipoplexes, which have been extensively used as nanocarriers for RNA delivery [29]. However, cationic nanoparticles are well known for their cellular toxicity, aggregation with serum proteins, and unspecific uptake by different cells, which pose serious concerns for *in vivo* use [30].

In the present study, we exploited the cationic nature of protamine, a naturally occurring low molecular weight protein, to form a condensed complex with anti-SNCA siRNA, which was subsequently mixed with anionic and neutral lipids to form negatively charged pegylated liposomes. The nanovesicles were modified with an RVG peptide to facilitate CNS distribution after intravenous administration, providing the potential for a non-invasive and convenient delivery route. The ability of liposomes to load and protect siRNA was tested with their ability to deliver siRNA and silence α-syn in mouse primary neuronal cell cultures.

The purpose of this work was to obtain a nanocarrier for siRNA delivery, which could be suitable for future *in vivo* applications, without the known undesirable features (e.g., positive charge and use of viral vectors) and with the advantages of simplicity, reproducibility, and safety of the formulation.

2 Experimental

2.1 Materials

Distearoylphosphatidylcholine (DSPC) and distearoylphosphatidylethanolamine-polyethyleneglycol-2000 (DSPE-PEG) were purchased from Lipoid (Ludwigshafen, Germany). Distearoylphosphatidylethanolamine-N-[maleimide(polyethylene glycol)-2000] (DSPE-PEG-Mal) was purchased from NOF corporation (Tokyo, Japan). Cholesterol, protamine, Liss-rhodamine, fluorescein amidite (FAM), and chloroform were purchased from Sigma-Aldrich (Milan, Italy). Amicon Ultra 4 concentrators (molecular weight cut-off (MWCO): 30 kDa) were purchased from Merck Millipore (Darmstadt, Germany). The RVG peptide with a cysteine on the C-terminal (YTIWMPENPRPGTPCDIFTNSRGKRASNGC) was synthesized by GenScript (Piscataway, NJ, USA).

The anti-SNCA siRNA (target sequence UGGCAACAGUGGCUGAGAA) and the negative control siRNA labeled with DY-547 (siGLO) were purchased from Dharmacon (Lafayette, CO, USA).

2.2 Protamine–siRNA complex formation and liposome preparation

Liposomes were prepared using the thin-film hydration method. For the preparation of stealth liposomes (SL), a mixture of DSPC (4.7 μmol), cholesterol (2.7 μmol),

and DSPE-PEG (0.4 μmol) was used. For the preparation of RVG-decorated liposome (RVGL), half of the DSPE-PEG was substituted with DSPE-PEG-Mal (0.2 μmol). The lipid mixture was dissolved in chloroform, which was then evaporated under reduced pressure at 25 ˚C to obtain a lipid film. The vacuum was applied for 6 h to ensure total removal of any solvent trace. In a separate vial, protamine and siRNA (anti-SNCA or fluorescent negative control, siGLO) were mixed at given ratios (Fig. 1) in RNAse-free phosphate-buffered saline (PBS, pH 7.4) and incubated for 30 min at room temperature with gentle stirring to allow formation of the complex. The lipid film was hydrated by mechanical stirring with the protamine–siRNA complexes (1.75 μg/mL siRNA) at 65 ˚C (above the transition temperature of DSPC, 55 ˚C). The liposomes obtained were sonicated using a Soniprep 150 ultrasonic disintegrator (MSE, London, UK) for 3 min with a scheme of pulses and pauses of 5 and 2 s, respectively. For the preparation of RVGL, RVG peptide (0.2 μmol) was incubated with maleimide-grafted liposomes overnight at room temperature. RVGL was separated from uncoupled peptide by centrifugal ultrafiltration (MWCO: 30 kDa). For the preparation of FAM and Liss-rhodamine-labeled stealth or RVG liposomes, the lipophilic dye Liss-rhodamine was included in the lipid mixture, while the hydrophilic dye FAM was included in the PBS hydration medium (pH 7.4). The concentration of each dye in the obtained liposome suspension was 50 μg/mL. Empty liposomes (EL) were prepared using the same lipid composition of SL in PBS hydration medium (pH 7.4).

2.3 Liposome physicochemical characterization: Mean size, polydispersity index, and zeta potential

The average diameter, polydispersity index (PDI), and zeta potential (ZP) of the samples were determined by photon correlation spectroscopy (PCS) using a Zetasizer Nano ZS (Malvern Instruments, Malvern, UK). Samples were backscattered by a helium–neon laser (633 nm) at an angle of 173° and a constant temperature of 25 ˚C. The instrument automatically adapts to the sample by adjusting the intensity of the laser and the attenuator of the photomultiplier, thus ensuring reproducibility of the experimental measurement conditions. The PDI was used as a measure of the width of the size distribution. PDI less than 0.2 indicates a homogenous and monodisperse population. Zeta potential was estimated using the Zetasizer Nano ZS by means of the M3-PALS (phase analysis light scattering) technique, which measures the particle electrophoretic mobility in a thermostated cell.

2.4 Encapsulation efficiency

The percent entrapment of siRNAs within liposomes was determined through an indirect fluorimetric method. Briefly, SL or RVGL were subjected to ultrafiltration using Amicon Ultra centrifugal filters (MWCO: 30 kDa). The free siRNA in the filtrate was quantified using the Quant-iT RiboGreen RNA assay (Invitrogen, Carlsbad, CA, USA) against an siRNA standard curve. The siRNA-RiboGreen fluorescence was measured with a microplate reader (Synergy 4, Bio-Tek, Winooski, VT, USA) using excitation and emission wavelengths of 495 and 525 nm, respectively.

2.5 Stability of vesicles in serum

SL and RVGL at 0.58 mg/mL total lipid concentration were incubated in 10% fetal bovine serum (FBS) at 37 ˚C with gentle agitation. At given time points, 200 μL of the incubation mixture was withdrawn and diluted with 800 μL distilled water. Size and PDI were measured by PCS at 37 ˚C immediately after the dilution.

2.6 Nuclease protection assay

To monitor the degradation of liposomal siRNA by serum nucleases, SL and RVGL were prepared at a final siRNA concentration of 133 nM and incubated with RNAse ONE (Promega, Fitchburg, WI, USA) at 37 ˚C. At the stated time points, 80 μL aliquots were removed, heated at 80 ˚C for 5 min to inactivate RNAses, mixed with sodium dodecyl sulfate (SDS, 0.5%) to disrupt liposomes, and stored at –80 ˚C until gel electrophoresis was performed. All samples were mixed with 10X BlueJuice gel loading buffer (Invitrogen) and were added to the wells of 1% agarose electrophoretic gel prepared with tris borate EDTA (TBE) buffer containing 6 μL Sybr Green II (Thermo Fisher Scientific, Waltham, MA, USA) per 100 mL solution.

The electrophoresis was carried out at 90 V for 45 min in TBE buffer. Unbound siRNA was used as a control. The bands were visualized via ultraviolet (UV) light using DNR Bioimaging Systems MiniBis Pro (Neve Yamin, Israel) and Image Lab 4.0.1 (Bio-Rad, Hercules, CA, USA). The relative amount of siRNA at each time point was quantified using the band at time 0 as a reference (100%).

2.7 Cell cultures

Primary cortical and hippocampal neuronal cell cultures were prepared from P0 newborn C57BL/6J mice. Brain cortices and hippocampi were dissected and mechanically dissociated in complete medium composed of Neurobasal A (Life Technologies, Milan, Italy) supplemented with 100 μg/mL penicillin, 100 μg/mL streptomycin (Sigma-Aldrich, Milan, Italy), 0.5 mM glutamine (EuroClone, Milan, Italy), and 1% B27 supplement (Gibco, Thermo Fisher Scientific, Waltham, MA, USA) and centrifuged. Cell count and viability assays were performed using the trypan blue exclusion test. For immunocytochemistry (ICC) or western blotting (WB) analysis, neurons were seeded either on poly-D-lysine-coated 24-well plate glass coverslides (8×10^4 cells/cm^2) or on poly-D-lysine-coated Petri dishes (4×10^5 cells/cm^2), respectively. Cells were maintained in complete medium at 37 °C in a humidified atmosphere of 5% CO_2 and 95% O_2 for 7 days *in vitro* prior to liposome treatment.

2.8 Liposome treatment

Cells were maintained in complete medium with liposomes containing a total of 25 nM α-syn siRNA at 37 °C in a humidified atmosphere of 5% CO_2 and 95% O_2 for 72 h. RVG empty liposomes were used at the same dilution as stealth liposomes. Control cells were maintained in complete medium under the same atmospheric conditions for 72 h.

In a subset of experiments, the cells were subjected to RNAi by using the conventional transfection agents INTERFERin (Polyplus-transfection, Illkirch, France) and Lyovec (InvivoGen, San Diego, CA, USA).

2.9 Immunocytochemistry

For immunostaining experiments, cells were fixed by incubation in 4% paraformaldehyde/4% sucrose in 1 M PBS (pH 7.4) for 10 min and then stored in PBS containing 0.05% sodium azide. Slides were incubated for 4 h at room temperature (RT) in blocking solution (1% *w*/*v* bovine serum albumin (BSA) plus 10% *v*/*v* normal goat serum (NGS) in PBS) then overnight at 4 °C with the primary antibody (SYN1, BD Biosciences, San Jose, CA, USA) at the optimal working dilution. On the following day, cells were incubated for 1 h at RT with the fluorescent secondary antibody diluted in 0.1% Triton X-100 PBS plus 1 mg/mL BSA. Finally, cell nuclei were counterstained either with 4′,6-diamidino-2-phenylindole (DAPI) (Sigma-Aldrich), Hoechst 33342 (Sigma-Aldrich), or ToPro (Invitrogen), and the coverslides were mounted on glass slides with Vectashield mounting medium for fluorescence (Vector Laboratories, Burlingame, CA, USA).

2.10 Antibodies

Alpha-synuclein was visualized using SYN-1 monoclonal antibodies (BD Biosciences, Milan, Italy). A mouse monoclonal anti-Neu-N antibody (Merck Millipore) was used for recognizing neuronal cells.

2.11 Statistical analysis

All statistical analyses were carried out with one-way ANOVA + Newman-Keuls post-comparison test.

3 Results and discussion

3.1 Liposome preparation and characterization

The liposomes were prepared using the thin-film hydration method. Neutral (DSPC, cholesterol) and anionic (DSPE-PEG, DSPE-PEG-Mal) lipids were selected with the aim of producing negatively charged vesicles. The EL were prepared by hydrating the lipid film with PBS (pH 7.4) and were used to optimize the lipid ratios and their total concentration. The mean diameter of the selected EL was 105 ± 5 nm with a *Z* potential of –31 ± 3 mV.

To exploit the negative charge of the liposomes as a driving force for siRNA loading, a cationic complex of siRNA and protamine was prepared. The protamine/siRNA mass ratio was optimized to achieve a stable positive charge and complete siRNA binding, which was confirmed via gel electrophoresis. A protamine/siRNA ratio of 1 was sufficient to associate all siRNA

and to form complexes with *Z* potential of 22 ± 4 mV (Fig. 1).

For the preparation of SL and RVGL, the lipid film was hydrated with a buffered solution containing siRNA-protamine complexes above the transition temperature of the main lipid, which equals 55 °C for DSPC. Therefore, the loading step was concurrent with the liposome formation, which was previously reported to achieve higher entrapment efficiency compared with the mixing of siRNA with preformed hollow liposomes [31]. To reduce liposome size and obtain small unilamellar vesicles (SUV), the formulations were subjected to sonication with a titanium probe sonicator. For the preparation of the RVGL, DPSE-PEG was partially substituted with DSPE-PEG-Mal, and after the sonication step, the RVG peptide was linked to the maleimide moieties exposed on the liposomal surface through the formation of a thioether bond. This reaction was carried out in PBS for 12 h at 25 °C with gentle stirring. To remove the uncoupled peptide from the RVGL dispersion, the crude product was filtered by centrifugal ultrafiltration (MWCO: 30 kDa) as previously described [32]. The purification step was necessary to rule out any possible competition between free RVG and RVGL for receptor binding. Moreover, since the maleimide group slowly undergoes hydrolysis when in contact with water, it was essential to proceed quickly in the preparation of RVGL.

A monodisperse population of liposomal nanoparticles (PDI < 0.2) was obtained with no significant ($P < 0.05$) difference in the size of the EL compared with that of the SL (105 ± 5 nm and 108 ± 8 nm, respectively). The size of the resulting liposomes before the reaction with the RVG peptide was similar to the size of SL, which confirms that the maleimide moiety does not induce aggregation nor destabilization of the bilayer.

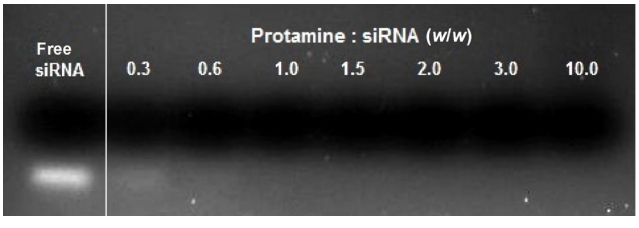

Figure 1 Electrophoretic gel of protamine–siRNA complexes at various weight ratios. Free siRNA (not complexed with protamine, first lane on the left) was used as a positive control.

Conversely, the mean diameter of the RVGL measured after the RVG peptide link to the vesicular surface was slightly increased (121 ± 4 nm), suggesting that covalent binding with maleimide occurred (Table 1). Moreover, the *Z* potential of RVGL significantly decreased after the reaction between the maleimide-grafted liposomes and the RVG peptide. A possible explanation could be that the RVG peptide has a calculated isoelectric point of 8.8, which translates to a net positive charge at pH 7.4, reducing the *Z* potential to −16 ± 5 mV. The formulated vesicles were separated from the free siRNA by centrifugal ultrafiltration to determine the entrapment efficiency, which resulted in 89% ± 4% for SL and 86% ± 4% for RVGL.

3.2 Nuclease protection assay

One of the main bottlenecks in the clinical use of siRNAs is their poor stability due to enzymatic degradation. Therefore, the ability of the liposomal formulation to protect loaded siRNAs against RNAses over time was tested *in vitro*. The SL were co-incubated with RNAse ONE at 37 °C, and sampling from the mixture was carried out at given time points. After the heat-mediated inactivation of RNAses, the siRNA was released from the nanocarriers by the addition of SDS. The anionic surfactant SDS was chosen to achieve the dual goal of disrupting the lipid vesicles and releasing the siRNA from protamine complexes to allow its migration and visualization on the electrophoretic gel. As shown in Fig. 2, the liposomal siRNA was sufficiently protected from enzymatic activity for a significantly longer time compared with naked siRNA (negative control, second lane), which was completely degraded after 10 min of incubation with RNAses. In Fig. 2(b), the relative amount of intact siRNA over time is reported. The quantitative analysis was carried out assuming as 100% the siRNA signal intensity at the beginning of the experiment (time 0)

As indicated by the graph, the black line (representing the liposomal siRNA) shows an initial burst of siRNA degradation (from 0 to 10 min), followed by a slowdown of the process rate. This could be ascribable to an immediate degradation of the free siRNA, followed by a second phase when the

Table 1 Mean diameter, PDI, and *Z* potential of EL, SL, and RVGL

Material	Mean diameter (nm)	PDI	*Z* potential (mV)	Encapsulation efficiency
EL	105 ± 5	0.129 ± 0.019	–31 ± 3	nd
SL	108 ± 8	0.131 ± 0.023	–28 ± 5	89% ± 4%
RVGL - before RVG binding	106 ± 5	0.153 ± 0.027	–30 ± 4	nd
RVGL - after RVG binding	121 ± 4	0.168 ± 0.022	–16 ± 5	86% ± 4%

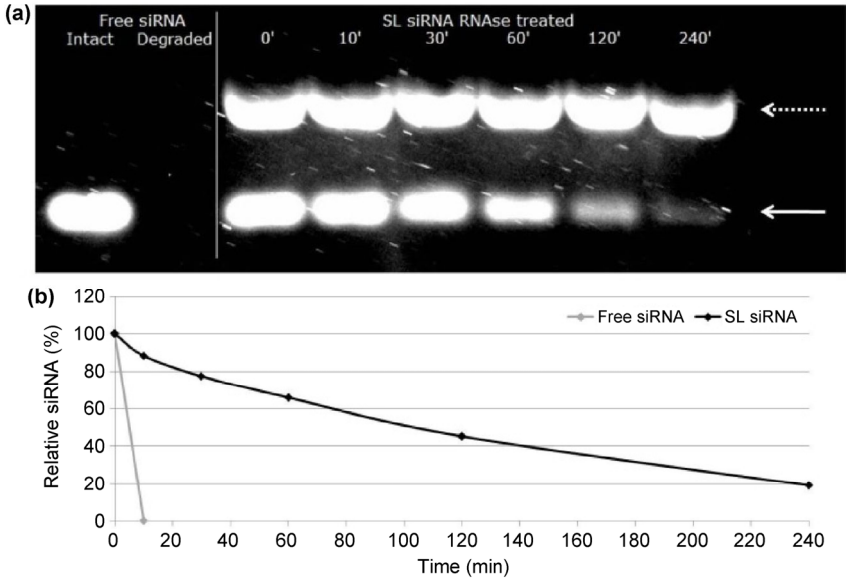

Figure 2 Nuclease protection assay. (a) Electrophoretic gel: On the left, free siRNA was either directly loaded on the gel (first lane, intact) or incubated with RNAses for 10 min (second lane, degraded) and used as positive or negative control, respectively. On the right, SL at different incubation times with RNAses (0, 10, 30, 60, 120, and 240 min) were disrupted with SDS to allow the visualization of encapsulated siRNA on the gel (white arrow). The dotted arrow indicates the signal of SDS. (b) The relative amount of intact siRNA is plotted against incubation time with RNAses. Black line: liposomal siRNA; grey line: free siRNA.

siRNA is slowly being released by the liposomes and thus becoming available for the enzymatic digestion. The brightest band present in all the SL lanes accounts for the signal of SDS, as confirmed by a control experiment with the surfactant alone (data not shown).

3.3 Serum stability

With the aim of future *in vivo* applications of our liposomal nanocarriers for siRNA delivery, the SL and RVGL were tested for their stability in 10% FBS. Indeed, although pegylation should confer "stealth" properties to avoid opsonization, this assay was necessary to rule out the possibility of an interaction between the RVG residues exposed on the surface of RVGL and serum proteins, which would promote aggregation of the nanoparticles resulting in a dramatic increase of the mean diameter [33]. As expected, the SL did not show any significant increase in size after 24 h of incubation with FBS. Interestingly, the RVGL also retained their initial diameter when exposed to FBS (Fig. 3). These results confirm that the length of the PEG chains and the DSPE-PEG/DSPC/cholesterol ratio were optimal to protect the liposomes from serum protein adsorption. Notably, the stealth properties were not lost following substitution of half the DSPE-PEG with DSPE-PEG-RVG for active targeting.

3.4 Uptake of liposomes and siRNA by primary mouse cortical neurons

In order to study the *in vitro* uptake of RVG and stealth liposomes by neuronal cells, we evaluated the internalization of FAM/Liss-rhodamine-labelled

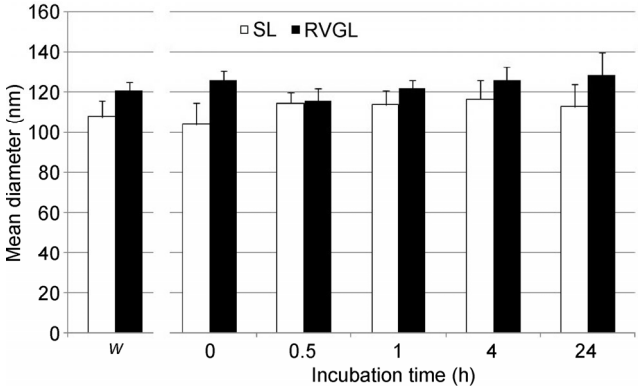

Figure 3 Vesicle stability in serum. The histogram represents the mean diameter of SL (white bars) or RVGL (black bars) after 0, 0.5, 1, 4, or 24 h incubation in 10% FBS. *W*: Mean diameter of SL and RVGL measured in water, to be used as a reference. Bars represent the mean ± standard deviation of at least three independent experimental determinations.

liposomes in primary mouse cortical neurons using confocal microscopy. Results show that neuronal cells internalized both FAM/Liss-rhodamine-labeled RVG and stealth liposomes (Fig. 4(a)). The presence of a marked FAM- and Liss-rhodamine-positive signal within cells in the higher magnification images confirms that several neurons were able to uptake large amounts of liposomes. In addition, the co-localization of the lipophilic and hydrophilic dyes within the cells corroborate the hypothesis that liposomes can cross the cell membrane while retaining their core–shell structure (Fig. 4(a), higher magnification). This observation correlates well with an uptake mechanism mediated by an endocytic pathway rather than by the fusion of the vesicles with the cell membrane.

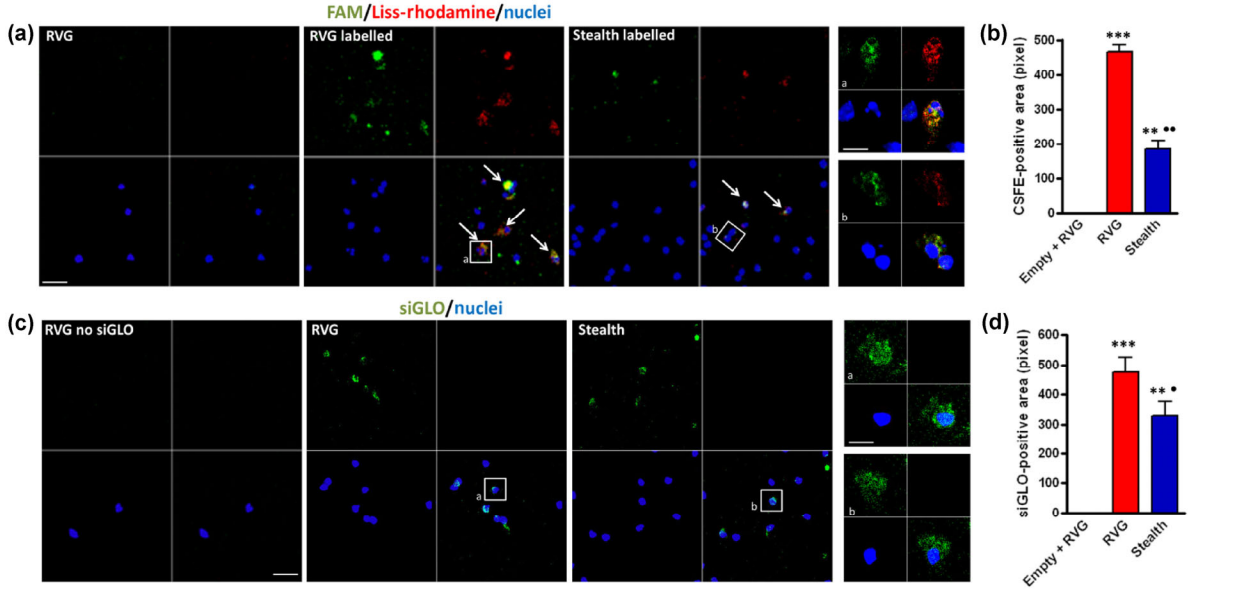

Figure 4 (a) Confocal microscopy images of FAM/Liss-rhodamine immunofluorescence in primary mouse cortical neurons exposed to control unlabeled RVG liposomes, FAM/Liss-rhodamine-loaded RVGL, or SL for 4 h. Cell nuclei were counterstained with Hoechst 33342. The presence of green and red fluorescence is indicative of FAM and Liss-rhodamine uptake, respectively. Scale bar: 50 μm; higher magnification scale bar: 15 μm. (b) Histogram of the mean ± standard error of the mean (SEM) of FAM-positive area in the primary cortical neurons treated with unlabeled RVGL, FAM/Liss-rhodamine-labeled RVGL, or SL. Neurons treated with the labeled RVG liposomes showed a marked increase of FAM-positive area (*** $P < 0.001$) compared with that of unlabeled RVGL-treated neurons that were devoid of green fluorescence signal. The neurons treated with the labeled SL also showed a statistically significant increase of FAM-positive area compared with that of unlabeled RVGL-treated cells (** $P < 0.01$), although this increase was significantly lower than that observed in labeled RVGL-treated cells (•• $P < 0.01$). (c) Confocal microscopy images of primary neuronal cell cultures treated for 4 h with empty RVGL or RVGL and SL loaded with siGLO. The green fluorescence signal is indicative of cell uptake of oligonucleotide duplexes. Scale bar: 50 μm; higher magnification scale bar: 15 μm. (d) Histogram of the siGLO-positive area ± SEM measured from primary neuronal cell cultures that were treated with empty RVGL or siGLO-loaded RVGL and SL for 4 h. Note the statistically significant increase of siGLO-positive area in the neurons treated with siGLO-loaded RVG liposomes compared with that of neurons treated with control RVG liposomes (*** $P < 0.001$). The neurons treated with siGLO-loaded SL also showed a significant increase of fluorescence compared with that of empty RVGL-treated cells (** $P < 0.01$). However, they showed a significantly lower positivity for siGLO compared with that of the neurons that were exposed to siGLO-loaded RVG liposomes (• $P < 0.05$).

The absence of FAM/Liss-rhodamine positivity in the control neurons treated with unlabeled RVG liposomes was indicative of the specificity of the positive fluorescence signal. Image analysis of FAM-positive areas (Fig. 4(b)) showed the increased uptake of FAM/Liss-rhodamine RVG liposomes in primary cortical neurons compared with that of unlabeled RVG liposomes and FAM/Liss-rhodamine-loaded stealth liposomes.

In addition, primary mouse cortical neurons were exposed to either RVG or stealth liposomes that had been previously loaded with siGLO green transfection indicator, a fluorescent oligonucleotide duplex. Neurons treated with empty RVG liposomes were used as controls. We observed that neurons treated with siGLO-loaded RVG liposomes could uptake fluorescently labeled oligonucleotide duplexes, whose signal was concentrated within cell nuclei as observed in the higher magnification panels (Fig. 4(c)). The neurons treated with siGLO-loaded stealth liposomes also showed positivity that seemed to be more diffused and less localized within the nuclei (Fig. 4(c)). This evidence suggests that, as expected, siRNA delivery by stealth liposomes had a slower uptake compared with that mediated by RVG liposomes. The specificity of the fluorescence signal was confirmed by the absence of positivity in the neurons exposed to siGLO-free RVG liposomes (Fig. 4(c)). These data were confirmed via image analysis (Fig. 4(d)) showing the presence of higher siGLO-positive area in siGLO-loaded RVGL compared with that of siGLO-loaded SL.

To corroborate that liposomes were actually internalized by neuronal cells and not by astrocytes, which were not prevalent in the primary neuronal cell cultures, neurons were exposed to either control empty RVG, FAM/Liss-rhodamine-labeled RVG, or FAM/Liss-rhodamine-labeled stealth liposomes for 4 h and then fixed and immunolabelled with the specific marker NeuN that marks the nuclei of neuronal cells. Consistent with our previous observations, we observed a higher uptake of FAM/Liss-rhodamine-labeled RVG and stealth liposomes by NeuN-positive cells (Fig. 5(a)), which was confirmed by the image analysis data of the number of NeuN/FAM-positive cells per mm^2 (Fig. 5(b)).

Finally, we probed the uptake of siGLO oligonucleotides enclosed in either RVG or stealth liposomes in the NeuN-immunolabeled primary neuronal cell cultures, with empty RVG liposomes used as a negative control for the green fluorescence signal (Fig. 5(c)). The results showed an increased uptake of siGLO in NeuN-positive neurons exposed to RVGL compared with that of neurons exposed to SL, as confirmed by image analysis (Fig. 5(d)).

Collectively, these results indicate that both RVG and stealth liposomes were internalized and could efficiently deliver siRNAs to primary cortical neurons. However, a difference in the intracellular localization exists between RVGL and SL, with the former showing a significantly higher uptake in all tested conditions. The increased uptake of RVGL is ascribable to the presence of the RVG peptide, which triggers endocytosis through the binding with nicotinic acetylcholine receptors that are present on the neuronal cell membranes [34].

3.5 Evaluation of liposome toxicity by Hoechst 33342 staining

To evaluate the toxicity of the liposomes, neurons were exposed to empty RVG, α-syn-specific siRNA-loaded RVGL, or SL for 72 h. Neurons subjected to medium additions of corresponding volumes at the same time of liposome treatments were used as a control (Figs. 6(a) and 6(b)). Interestingly, we found that neurons exposed to siRNA-loaded SL showed a higher number of condensed nuclei that are indicative of apoptotic cells compared with that of the control and empty RVG- or siRNA-loaded RVGL-exposed neurons. These results indicate that although SL can efficiently deliver siRNAs into neurons, their use is associated with toxicity. A possible explanation for the fact that SL was more toxic than RVGL may be that they induce more severe damage to neuronal cell membranes. Although the uptake of SL is lower than that of RVGL, SL uptake is mediated by non-specific mechanisms that might disrupt neuronal membrane homeostasis. This hypothesis is consistent with previous studies reporting the membrane toxicity of liposomal transfection reagents in primary neuronal cell cultures [35].

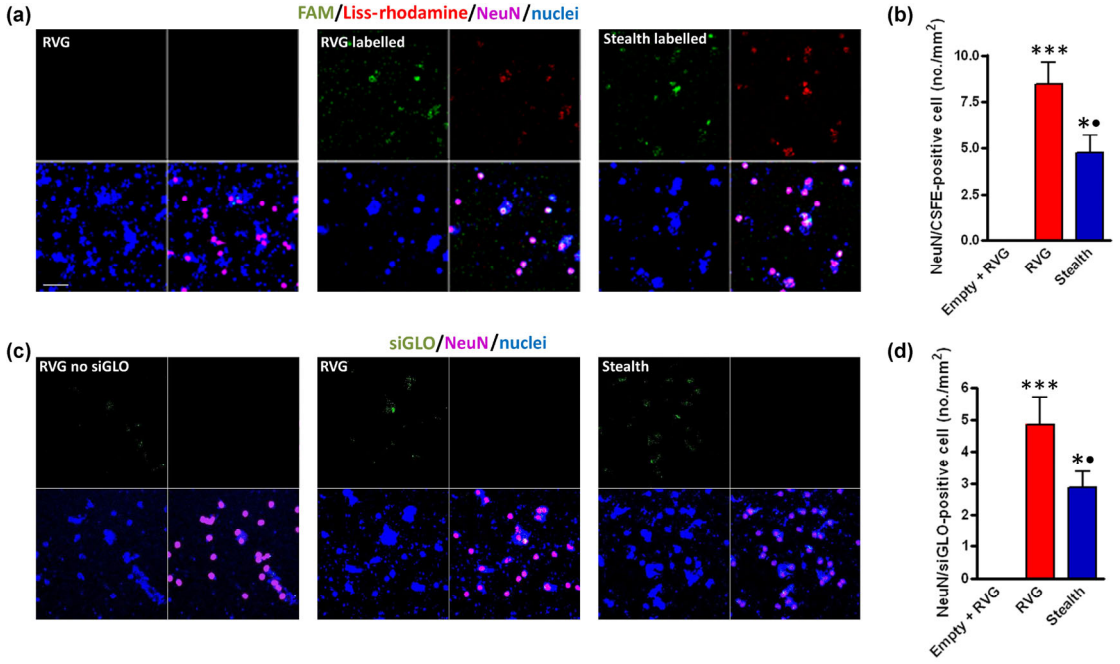

Figure 5 (a) Confocal microscopy images of FAM/Liss-rhodamine immunofluorescence in NeuN-immunopositive cortical neurons exposed for 4 h to unlabeled RVGL, FAM/Liss-rhodamine-loaded RVGL, or SL. Scale bar: 50 µm. (b) Histogram of the mean ± SEM of FAM/NeuN-positive cells per mm^2 in the cortical neuron cultures exposed for 4 h to unlabeled RVGL and FAM/Liss-rhodamine-labeled-RVGL or SL. There was a statistically significant increase in the number of FAM/NeuN-positive cells in the cultures that were exposed to FAM/Liss-rhodamine RVG liposomes (*** $P < 0.001$) compared with that of unlabeled RVGL-treated neurons. The neurons exposed to FAM/Liss-rhodamine SL also showed a statistically significant increase of FAM-positive area compared with that of unlabeled RVGL-treated cells (* $P < 0.05$), although this increase was significantly lower than that observed in the cells treated with FAM/Liss-rhodamine RVG liposomes (• $P < 0.05$). (c) Confocal microscopy images of NeuN-immunopositive neuron cultures treated for 4 h with empty RVGL or RVGL and SL loaded with siGLO. The green fluorescence signal is indicative of the cell uptake of oligonucleotide duplexes. Scale bar: 50 µm. (d) Histogram of the mean ± SEM of siGLO/NeuN-positive neurons in the primary cortical cultures that were treated for 4 h with empty RVG and siGLO-loaded RVGL or SL. The cells exposed to siGLO-loaded RVGL showed a statistically significant increase of siGLO/NeuN-positive neurons compared with that of cells treated with empty RVGL (*** $P < 0.001$). The neurons treated with the siGLO-loaded SL also showed a significant increase of siGLO/NeuN-positive cells compared with that of empty RVGL-treated cells (* $P < 0.05$). However, a significantly lower number of siGLO/NeuN-positive cells were observed compared with the number of neurons exposed to siGLO-loaded RVG liposomes (• $P < 0.05$).

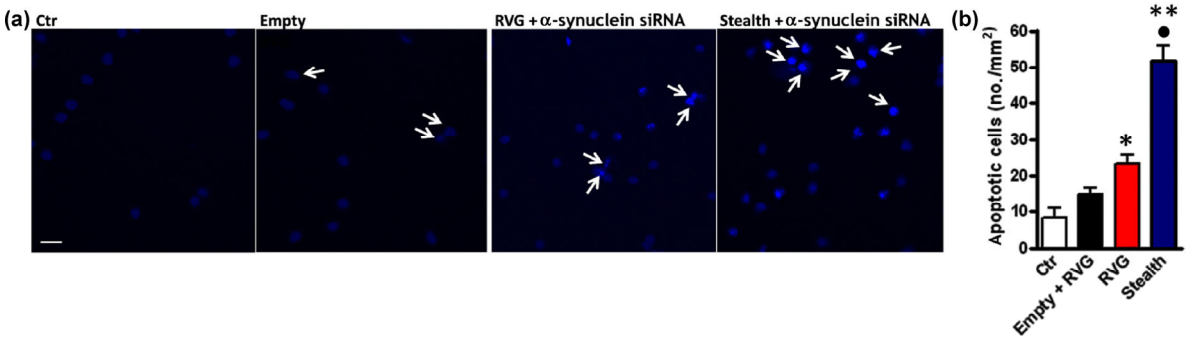

Figure 6 (a) Representative photomicrographs of Hoechst 33342 labeling in primary cortical neuron cultures in basal condition (Ctr) or after a 72 h exposure to empty RVGL or RVGL and SL loaded with α-synuclein siRNA. Note the presence of several nuclei with condensed chromatin (arrows) that is indicative of apoptotic cells. Scale bar: 50 µM. (b) Histogram of the number of apoptotic cells evaluated by counting the number of nuclei with condensed chromatin per mm^2. A slight although statistically significant increase of apoptotic cells was evident in the neurons that were treated with RVG liposomes loaded with siRNA compared with that of neurons treated with empty RVG liposomes (* $P < 0.05$). The use of SL loaded with siRNA was associated with a statistically significant increase in the number of apoptotic cells compared with that of both empty RVG (** $P < 0.01$) and siRNA-loaded RVG liposomes (• $P < 0.05$).

3.6 Evaluation of the efficiency of liposome-mediated α-syn gene silencing in mouse primary cortical and hippocampal neurons

Finally, we evaluated whether RVG and SL loaded with 25 nM of the siRNA sequence previously used to induce α-syn gene silencing in mouse primary neurons [36] could be used to efficiently silence this protein in cortical and hippocampal neuronal cell cultures. Neurons exposed to empty RVG liposomes or transfected with common siRNA-delivery agents such as INTERFERin and Lyovec were used as controls. Efficiency of α-syn gene silencing was probed by analyzing the α-syn-immunopositive area. Indeed, we previously described a discrepancy between mRNA and protein levels measured by real-time polymerase chain reaction (PCR) and western blotting, respectively, in neurons exposed to α-syn siRNA [35]. Moreover, immunocytochemical analysis offers the possibility to probe α-syn expression, assess its distribution in neuronal cells, and probe neuronal viability by Hoechst 33342, thus offering a valuable method to efficiently assess gene silencing and avoid false results derived from neuronal cell cultures that degrade upon liposome exposure.

We found a marked reduction in the α-syn-immunopositive signal in primary cortical neurons exposed to siRNA-RVGL compared with that of both control and empty RVG liposomes (Figs. 7(a) and 7(c)). Additionally, the efficiency of α-syn gene silencing by siRNA-RVGL was comparable to that observed when siRNA was transfected with either Lyovec or INTERFERin. Conversely, stealth liposomes loaded with siRNA were only able to induce a 40% reduction of α-syn levels compared with that of either control or empty RVG-treated cells; this difference was statistically significant compared to the response in siRNA-RVGL-exposed neurons.

These data were confirmed by using primary hippocampal neuronal cell cultures that are usually affected by LB pathology in DLB (Figs. 7(b) and 7(d)). We found a marked decrease of α-syn-immunopositive signal in the hippocampal neurons exposed to siRNA-RVGL compared with that in control or empty RVG

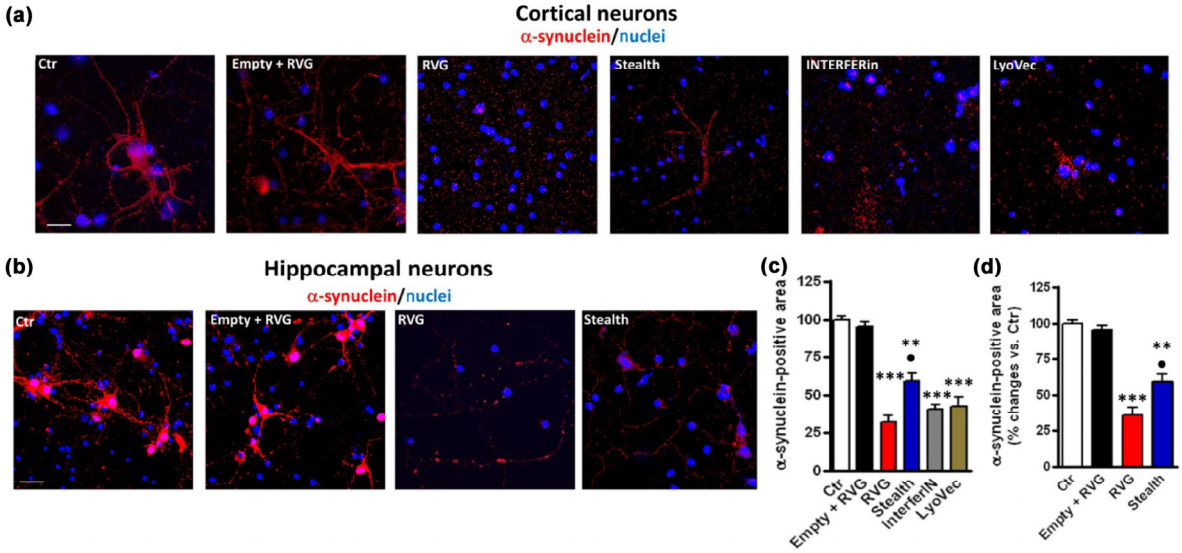

Figure 7 (a) Images of alpha-synuclein immunolabeling in primary cortical neurons in basal conditions (Ctr), exposed to empty RVG liposomes, or subjected to alpha-synuclein gene silencing by using an siRNA concentration of 25 nM delivered by RVGL, SL, INTERFERin, or Lyovec. (b) Representative photomicrographs of primary hippocampal neuron cultures in basal conditions (Ctr) and exposed to empty RVG liposomes, RVGL, or SL loaded with 25 nM alpha-synuclein siRNA. (c) Graph of the mean ± SEM of alpha-synuclein-immunopositive area in the primary mouse cortical neurons represented in panel a. Note the marked reduction of alpha-synuclein-immunopositive area in the neurons subjected to gene silencing by RVG liposomes, INTERFERin, and Lyovec compared with that of empty RVG-exposed neurons (*** $P < 0.001$). In the cultures exposed to alpha-synuclein siRNA-loaded SL, the immunopositive area was significantly higher compared with that of the cells in which gene silencing was mediated by other transfection agents (• $P < 0.05$), and it was significantly different from that of empty RVG-treated neurons (** $P < 0.01$) (d) Graph of the mean ± SEM of alpha-synuclein-immunopositive area in the primary mouse hippocampal neurons represented in panel b.

liposomes. However, siRNA-SL resulted in a lower reduction of α-syn levels compared with that of siRNA-RVGL, which is in accordance with the results obtained from primary cortical neurons.

Since the use of SL was associated with higher toxicity compared with that of RVGL, it is plausible that their reduced ability to induce α-syn gene silencing is due to the fact that the impairment of cell viability is responsible for the reduction of siRNA efficiency.

These results indicate that RVG liposomes loaded with α-syn siRNA can induce an efficient and reproducible reduction of the protein in mouse neuronal cells and could likely be tested as promising and efficient delivery agents for siRNA *in vivo* mouse models.

4 Conclusions

The anionic liposomes decorated with the brain-targeting RVG peptide were capable of efficiently loading, protecting, and delivering anti-α-syn siRNA to primary cortical and hippocampal cells *in vitro*. Once released inside the neuronal cells, the siRNA significantly reduced the levels of α-syn without affecting cell viability. The purpose of this research was to produce a formulation that is stable in serum and suitable for non-invasive administration *in vivo*. Moreover, the design of the nanocarrier followed a straightforward approach exploiting simple solutions to overcome the most common drawbacks in siRNA delivery. In summary, a simple formulation with marked *in vitro* efficacy was produced with potential to overcome the complex barriers encountered in the *in vivo* environment.

Acknowledgements

The authors gratefully acknowledge Micaela Morelli for supporting the establishment of the collaboration between the groups participating to this study. M. S. thanks Angela Corona for fruitful discussions about the design and implementation of the project. A. B. is grateful to "Ambrosini Arredamenti SNC" for funding support within the project "Molecular Mechanisms, associated with Neurodegenerative Diseases" and the Italian Ministry of Education, University and Scientific Research—University of Brescia Ex 60% Research Funds.

References

[1] Bendor, J. T.; Logan, T. P.; Edwards, R. H.The function of α-synuclein. *Neuron* **2013**, *79*, 1044–1066.

[2] McLean, P. J.; Kawamata, H.; Ribich, S.; Hyman, B. T. Membrane association and protein conformation of α-synuclein in intact neurons. Effect of parkinson's disease-linked mutations. *J. Biol. Chem.* **2000**, *275*, 8812–8816.

[3] Lashuel, H. A.; Overk, C. R.; Oueslati, A.; Masliah, E. The many faces of α-synuclein: From structure and toxicity to therapeutic target. *Nat. Rev. Neurosci.* **2013**, *14*, 38–48.

[4] Bellucci, A.; Mercuri, N. B.; Venneri, A.; Faustini, G.; Longhena, F.; Pizzi, M.; Missale, C.; Spano, P. Parkinson's disease: From synaptic loss to connectome dysfunction. *Neuropathol. Appl. Neurobiol.* **2016**, *42*, 77–94.

[5] Bellucci, A.; Zaltieri, M.; Navarria, L.; Grigoletto, J.; Missale, C.; Spano, P. From α-synuclein to synaptic dysfunctions: New insights into the pathophysiology of Parkinson's disease. *Brain Res.* **2012**, *1476*, 183–202.

[6] Maraganore, D. M. Rationale for therapeutic silencing of alpha-synuclein in Parkinson's disease. *J. Mov. Disord.* **2011**, *4*, 1–7.

[7] Specht, C. G.; Schoepfer, R. Deletion of the alpha-synuclein locus in a subpopulation of C57BL/6J inbred mice. *BMC Neurosci.* **2001**, *2*, 11.

[8] Spillantini, M. G.; Crowther, R. A.; Jakes, R.; Hasegawa, M.; Goedert, M. α-synuclein in filamentous inclusions of Lewy bodies from Parkinson's disease and dementia with Lewy bodies. *Proc. Natl. Acad. Sci. USA* **1998**, *95*, 6469–6473.

[9] Braak, H.; DelTredici, K.; Rüb, U.; de Vos, R. A.; Jansen Steur, E. N.; Braak, E. Staging of brain pathology related to sporadic Parkinson's disease. *Neurobiol. Aging* **2003**, *24*, 197–211.

[10] Eslamboli, A.; Romero Ramos, M.; Burger, C.; Bjorklund, T.; Muzyczka, N.; Mandel, R. J.; Baker, H.; Ridley, R. M.; Kirik, D.Long-term consequences of human alpha-synuclein overexpression in the primate ventral midbrain. *Brain* **2007**, *130*, 799–815.

[11] Uversky, V. N. Neuropathology, biochemistry, and biophysics of α-synuclein aggregation. *J. Neurochem.* **2007**, *103*, 17–37.

[12] Sapru, M. K.; Yates, J. W.; Hogan, S.; Jiang, L. X.; Halter, J.; Bohn, M. C. Silencing of human α-synuclein *in vitro* and in rat brain using lentiviral-mediated RNAi. *Exp. Neurol.* **2006**, *198*, 382–390.

[13] O'Mahony, A. M.; Godinho, B. M. D. C.; Cryan, J. F.; O'Driscoll, C. M.Non-viral nanosystems for gene and small interfering RNA delivery to the central nervous system: Formulating the solution. *J. Pharm. Sci.* **2013**, *102*, 3469–3484.

[14] Lewis, J.; Melrose, H.; Bumcrot, D.; Hope, A.; Zehr, C.; Lincoln, S.; Braithwaite, A.; He, Z.; Ogholikhan, S.; Hinkle, K. et al. *In vivo* silencing of alpha-synuclein using naked siRNA. *Mol. Neurodegener.* **2008**, *3*, 19.

[15] McCormack, A. L.; Mak, S. K.; Henderson, J. M.; Bumcrot, D.; Farrer, M. J.; Di Monte, D. A. α-synuclein suppression by targeted small interfering RNA in the primate substantia nigra. *PLoS One* **2010**, *5*, e12122.

[16] Gorbatyuk, O. S.; Li, S. D.; Nash, K.; Gorbatyuk, M.; Lewin, A. S.; Sullivan, L. F.; Mandel, R. J.; Chen, W. J.; Meyers, C.; Manfredsson, F. P. et al. *In vivo* RNAi-mediated α-synuclein silencing induces nigrostriatal degeneration. *Mol. Ther.* **2010**, *18*, 1450–1457.

[17] Nayak, S.; Herzog, R. W.Progress and prospects: Immune responses to viral vectors. *Gene Ther.* **2010**, *17*, 295–304.

[18] Li, C. X.; Parker, A.; Menocal, E.; Xiang, S. L.; Borodyansky, L.; Fruehauf, J. H. Delivery of RNA interference. *Cell Cycle* **2006**, *5*, 2103–2109.

[19] Haussecker, D. Current issues of RNAi therapeutics delivery and development. *J. Control. Release* **2014**, *195*, 49–54.

[20] Grimm, D. Small silencing RNAs: State-of-the-art. *Adv. Drug Deliv. Rev.* **2009**, *61*, 672–703.

[21] Yang, J.; Liu, H. M.; Zhang, X. Design, preparation and application of nucleic acid delivery carriers. *Biotechnol. Adv.* **2014**, *32*, 804–817.

[22] David, S.; Pitard, B.; Benoît, J. P.; Passirani, C. Non-viral nanosystems for systemic siRNA delivery. *Pharmacol. Res.* **2010**, *62*, 100–114.

[23] Cooper, J. M.; Wiklander, P. B. O.; Nordin, J. Z.; Al Shawi, R.; Wood, M. J.; Vithlani, M.; Schapira, A. H. V.; Simons, J. P.; El Andaloussi, S.; Alvarez Erviti, L. Systemic exosomal siRNA delivery reduced alpha-synuclein aggregates in brains of transgenic mice. *Mov. Disord.* **2014**, *29*, 1476–1485.

[24] Alvarez Erviti, L.; Seow, Y.; Yin, H. F.; Betts, C.; Lakhal, S.; Wood, M. J. A. Delivery of siRNA to the mouse brain by systemic injection of targeted exosomes. *Nat. Biotechnol.* **2011**, *29*, 341–345.

[25] Kumar, P.; Wu, H. Q.; McBride, J. L.; Jung, K. E.; Kim, M. H.; Davidson, B. L.; Lee, S. K.; Shankar, P.; Manjunath, N. Transvascular delivery of small interfering RNA to the central nervous system. *Nature* **2007**, *448*, 39–43.

[26] Robbins, P. D.; Morelli, A. E. Regulation of immune responses by extracellular vesicles. *Nat. Rev. Immunol.* **2014**, *14*, 195–208.

[27] Vader, P.; Mol, E. A.; Pasterkamp, G.; Schiffelers, R. M. Extracellular vesicles for drug delivery. *Adv. Drug Deliv. Rev.* **2016**, *106*, 148–156.

[28] De Luca, M. A.; Lai, F.; Corrias, F.; Caboni, P.; Bimpisidis, Z.; Maccioni, E.; Fadda, A. M.; Di Chiara, G. Lactoferrin- and antitransferrin-modified liposomes for brain targeting of the NK3 receptor agonist senktide: Preparation and *in vivo* evaluation. *Int. J. Pharm.* **2015**, *479*, 129–137.

[29] Ozpolat, B.; Sood, A. K.; Lopez Berestein, G. Liposomal siRNA nanocarriers for cancer therapy. *Adv. Drug Deliv. Rev.* **2014**, *66*, 110–116.

[30] Li, W. J.; Szoka, F. C. Lipid-based nanoparticles for nucleic acid delivery. *Pharm. Res.* **2007**, *24*, 438–449.

[31] Buyens, K.; Demeester, J.; De Smedt, S. S.; Sanders, N. N. Elucidating the encapsulation of short interfering RNA in PEGylated cationic liposomes. *Langmuir* **2009**, *25*, 4886–4891.

[32] Huo, H.; Gao, Y. K.; Wang, Y.; Zhang, J. H.; Wang, Z. Y.; Jiang, T. Y.; Wang, S. L. Polyion complex micelles composed of pegylated polyasparthydrazide derivatives for siRNA delivery to the brain. *J. Colloid Interface Sci.* **2015**, *447*, 8–15.

[33] Hamidi, M.; Azadi, A.; Rafiei, P. Pharmacokinetic consequences of pegylation. *Drug Deliv.* **2006**, *13*, 399–409.

[34] Lafon, M. Rabies virus receptors. *J. Neurovirol.* **2005**, *11*, 82–87.

[35] Bauer, M.; Kristensen, B. W.; Meyer, M.; Gasser, T.; Widmer, H. R.; Zimmer, J.; Ueffing, M. Toxic effects of lipid-mediated gene transfer in ventral mesencephalic explant cultures. *Basic Clin. Pharmacol. Toxicol.* **2006**, *98*, 395–400.

[36] Zaltieri, M.; Grigoletto, J.; Longhena, F.; Navarria, L.; Favero, G.; Castrezzati, S.; Colivicchi, M. A.; Della Corte, L.; Rezzani, R.; Pizzi, M. et al. α-synuclein and synapsin III cooperatively regulate synaptic function in dopamine neurons. *J. Cell Sci.* **2015**, *128*, 2231–2243.